Mush–liquid interfaces with cross flow

Devin Conroy

March 15, 2007

1 Introduction

The solidification of a binary melt growing into a supercooled region may lead to the formation of a mushy layer as a result of morphological instability of the plane boundary. Mushy layers are reactive porous media that suppress constitutional supercooling caused by the rejection of residual solute. When the rejected solute causes a statically unstable density stratification, compositional convection can occur, provided the Rayleigh number is large enough. Past experiments and theoretical results have shown that channels can form between convection cells, where fluid of high solute concentration has a maximum vertical velocity, which acts to dissolve the interior of the mushy layer. The channels grow in time, providing the path of least resistance for the continually convecting fluid, which is fed by the continual growth of solid and rejection of solute.

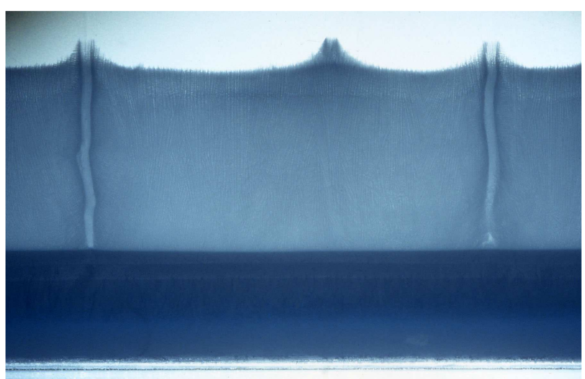

Figure 1: Mushy layer of ammonium chloride crystal grown from an aqueous solution, showing the structure of two complete chimneys. Taken from Worster (2000)

.

Fluid contained within the interior of a mushy layer, as shown in figure (1), is convected out through the chimneys and replaced by fluid from above. Along the walls of the chimney, fluid is then flowing from mush to liquid across a solidifying interface, and along the top of the mushy layer fluid is flowing from liquid to mush across a solidifying interface. Recently Schulze and Worster (1999, 2005) have examined the appropriate boundary conditions to be applied at these interfaces in order to determine the position of the mush–liquid interface. In general there are four separate cases corresponding to a solidifying or dissolving boundary and whether the flow of material is from mush to liquid or from liquid to mush. Three of those conditions have been explored using one-dimensional models but the fourth, which is the topic of this study, requires the flow to be at least two dimensional. The dissolving boundary occurs initially when the chimney first forms from a liquid inclusion but later on the walls of the chimney are actually in a solidifying regime. In this case the fluid is leaving the mush across a solidifying boundary and we want the time-rate of change of temperature following a material particle at the interface to be zero. This condition, which is equivalent to the isotherms being tangent to the streamlines, is a relatively new idea that still requires exploration in order to fully understand the nature and consequences of it.

2 Governing Equations

In this analysis we are looking at the configuration illustrated in figure 2 (see Le Bars et. al. 2006), which is a simplified model designed to explore the nature and consequences of a solidifying mush–liquid interface having material flowing from mush to liquid. It is a convenient way of exploring a 2–dimensional flow with a 1–dimensional analysis. In addition we require a 2-D temperature field in which the upper and lower boundary temperatures vary linearly with x in order to maintain the same mathematical structure as the stream function ψ. In addition we require the solid fraction and interface position to be independent of the horizontal distance x.

Fluid flows from the bottom boundary into the mushy layer at a velocity W_B and out of the top boundary at a velocity W_T, where $W_T \leq W_B$. Since we are strictly interested in the case in which the mushy layer is growing, we take the lower boundary to be colder than the upper boundary ($m_1 < m < m_2$), where m is the slope of the liquidus curve in the phase diagram. The mushy layer is solidifying at a rate $\mathrm{d}a/\mathrm{d}t$, where $a(t)$ is the position of the interface. In addition we are pulling the whole apparatus downwards at a constant speed V which will be equivalent to the growth rate of the mush–liquid interface in the non-moving reference frame at steady state.

2.1 Mushy Layer

Within the mushy layer ($0 < z < a$) we have a reactive porous medium that requires appropriately volume averaged equations for temperature, T and concentration, C. Here we assume that the ideal mushy layer equations apply (see Worster 1997), namely

$$\begin{aligned}
\frac{\partial T}{\partial t} + \mathbf{q}\cdot\nabla T &= \kappa\nabla^2 T + \frac{L}{c_p}\frac{\partial \phi}{\partial t} - \frac{VL}{c_p}\frac{\partial \phi}{\partial z}, && (1)\\
(1-\phi)\frac{\partial C}{\partial t} + \mathbf{q}\cdot\nabla C &= (C - C_s)\left(\frac{\partial \phi}{\partial t} - V\frac{\partial \phi}{\partial z}\right), && (2)\\
T &= T_L(C) = -m\,C, && (3)
\end{aligned}$$

where the diffusion of salt is assumed to be negligible and the temperature field in the mush is constrained to the concentration field by the liquidus relationship. Here $q = \mathbf{u} - V\hat{\mathbf{k}}$, κ is

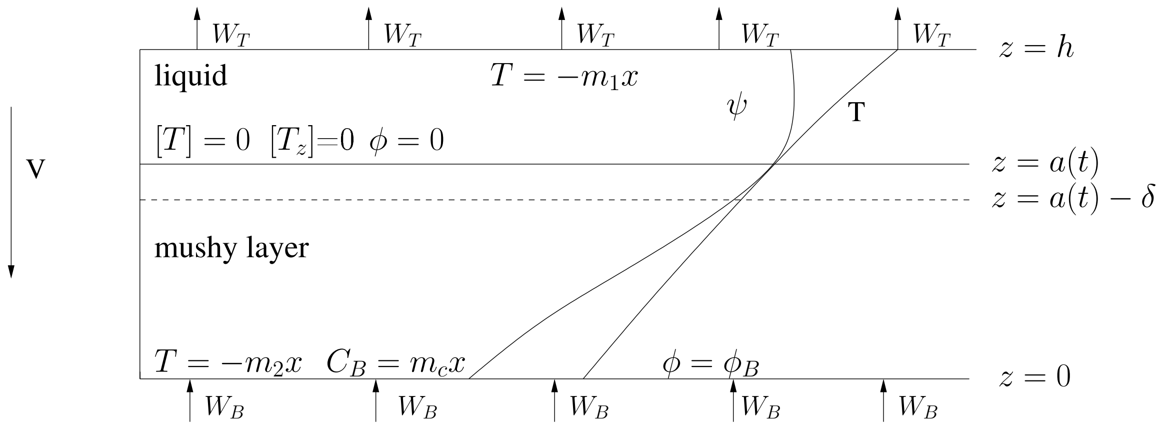

Figure 2: Diagram showing a channel of infinite length with a mushy layer contained in the region $z < a$ and a liquid layer above. There is a flow of relatively cool fluid from the bottom boundary at a rate W_B and a flow out of the channel at a smaller velocity, W_T. The left hand boundary is fresh, i.e. no solute, and non-permeable.

the thermal diffusivity, L is the latent heat, c_p is the specific heat, ϕ is the solid fraction and C_s is the concentration in the solid. In this analysis we will assume that the solid is pure, i.e. $C_s = 0$, and that the liquidus temperature T_L decreases linearly with solute concentration. At the bottom of the channel we assume that the temperature and bulk concentration vary linearly with distance x as

$$T(x, 0, t) = -m_2 x, \qquad C_{\text{bulk}}(x, 0, t) = (1 - \phi_B)\, C(T) = (1 - \phi_B)\, m_b x, \tag{4}$$

where $m_b = m_2/m$ is the slope of the solute concentration and ϕ_B is the lower boundary solid fraction that must be determined as part of the solution. It should be noted that the bulk concentration presented here comes from some outer solution and only applies when the q flow is from mush to liquid. If the flow is in the opposite direction then as we will see in the next section, the bulk concentration must be imposed at the upper surface.

2.2 Liquid Layer

In the liquid layer above the mush ($a < z < h$) we again assume that the diffusion of salt is negligible compared to advection and we use the following equations

$$\frac{\partial T}{\partial t} + \mathbf{q} \cdot \nabla T = \kappa \nabla^2 T, \tag{5}$$

$$\frac{\partial C}{\partial t} + \mathbf{q} \cdot \nabla C = 0. \tag{6}$$

At the upper surface we also assume that the temperature decreases linearly from the boundary $x = 0$ with the relationship

$$T(x, h) = -m_1\, x, \tag{7}$$

where the condition $m_1 < m < m_2$ must be imposed for a solidifying interface.

Since the concentration field is controlled by the advection equation and we have imposed a solid fraction at the lower boundary the concentration equation (6) is decoupled from the system provided that the q-flow is out of the top boundary. The concentration field, without the effect of diffusion, just follows the streamlines with the unknown mush–liquid concentration. On the other hand if the q flow is from liquid to mush then the advection of bulk concentration from the upper boundary must be used to determine the temperature at the mush–liquid interface. In this case we impose a bulk concentration at the upper boundary of the form

$$C_{\text{bulk}}(x,h) = C(T) = m_t\, x, \tag{8}$$

where the solid fraction is zero.

2.3 Interface Conditions

At the interface between the mush and liquid layers ($z = a$) we follow Worster (2000) and use the conditions

$$[T] = 0, \qquad [T_z] = 0, \qquad \phi = 0, \qquad z = a, \tag{9}$$

where the last one comes from the assumption that the diffusion of solute is negligible.

A subtle boundary condition presented in Schultz (2005) based on the complete removal of constitutional supercooling, requires that streamlines be tangent to isotherms in the case that fluid flows from the mush to the liquid across a solidifying boundary. This condition essentially means that the change in temperature moving with a material particle is zero at the interface, expressed mathematically as

$$\frac{D^q\,T}{D\,t} = 0 \rightarrow \frac{\partial T}{\partial t} + (\mathbf{u} - V\hat{k}) \cdot \nabla T = 0, \tag{10}$$

where q represents the mean velocity of the material particles, $\hat{k}$ is the unit vector in the vertical direction and we have shifted our coordinate system to move at the pulling speed V.

This condition can be justified by considering the change in temperature following a material particle, which according to the idea of equilibrium (see Worster 2000) will have the following property

$$\frac{D^q\,T}{D\,t} \geq \frac{D^q\,T_L(C)}{D\,t} \tag{11}$$

in the liquid at the mush–liquid interface $z = a$. In order to ensure that the liquid is not locally supercooled we require the change in solute concentration to be zero, $D^q\,T/D\,t = 0$ and from the liquidus condition this translates to $D^q\,T_L(C)/D\,t = 0$. Therefore a fluid particle moving at the mean velocity q must be warming up as it crosses the interface. On the mush side of the interface equation (2) can be expressed as

$$\frac{D^qC}{Dt} = \phi\frac{\partial C}{\partial t} + C\frac{D^v\phi}{Dt} \tag{12}$$

where the superscript v represent the mean velocity of the solid particles i.e. $D^v/D\,t = \partial/\partial t - V\hat{k}\cdot\nabla$. Since the solid fraction is zero at the mush–liquid interface the first term on the right-hand side is zero. For a solidifying mush the change in solid fraction with time moving with the solid must be increasing $D^v\,\phi/D\,t \geq 0$ and therefore equation (12) give the opposite condition

$$\frac{D^q\,T}{D\,t} \leq 0 \tag{13}$$

on the mush side of the interface. As long as the temperature gradients and velocities are continuous across this interface then equation (10) must be true.

2.4 Velocity Profiles

In the setup shown in figure (2) we assume that the velocity profiles have the same structure as the well known solution for a corner flow (e.g. Batchelor 1967) in the case of a pure fluid, which are given in terms of a stream function by

$$\mathbf{u} = (u, w) = \left(\frac{\partial\psi}{\partial z}, -\frac{\partial\psi}{\partial x}\right), \qquad \psi = -Vxf(z). \tag{14}$$

This formulation applies in both the mushy and liquid layers and allows us to satisfy continuity exactly in the case of a two-dimensional incompressible flow. We impose the following conditions on the boundaries of the domain

$$w(x,0) = W_B, \quad u(x,h) = 0, \quad w(x,h) = W_T, \quad \left.\frac{\partial u}{\partial z}\right|_{x,z=0} = 0 \tag{15}$$

where the last condition expresses no horizontal shear and is only used for the Darcy–Brinkman formulation (see below).

2.4.1 Stokes-Darcy Formulation

Darcy's equation is commonly used in the study of porous media and has had success when compared to experimental observation (See Bear 1972). Strictly the equation applies for a low Reynolds number flow when the permeability is sufficiently small, which is the case in most types of porous media. Outside the mushy layer we have a thin channel that obeys Stokes equation for a thin gap. These equations are

$$-\nabla P = \frac{\mu}{\Pi}\mathbf{u} \qquad 0 \leq z \leq a-\delta, \tag{16}$$

$$\nabla P = \mu\nabla^2\mathbf{u} \qquad a-\delta \leq z \leq h, \tag{17}$$

where the permeability Π is given by the following non-divergent function

$$\Pi = \Pi_0(1-\phi)^3, \tag{18}$$

in terms of the solid fraction ϕ and δ is the thickness of a transition zone to be explained next.

At the mush–liquid interface it is well known and expected that the pressure and vertical mass flux are continuous, although this is not necessarily the case for the horizontal velocity. Since we cannot interrogate the porous media very close to the interface there is a region of depth δ where Darcy's equation is not valid. In this region the pressure is balanced by both fluid–solid and fluid–fluid interactions, where the thickness of the transition zone δ then is defined to be the depth at which viscous dissipation at the solid walls dominate. Following Le Bars et.al. (2006) the depth of this transition zone is given by

$$\delta = c\sqrt{\frac{Da\, k_i}{1-\phi_i}}, \tag{19}$$

where c is a scaling coefficient $k = \Pi/\Pi_0$, $Da = \Pi/h^2$ is the Darcy number and subscript, i indicates the level $a - \delta$. Since this thickness is normally small, $\phi_i \ll 1$ and we can to leading order write this equation as

$$\delta \sim c\sqrt{Da}. \tag{20}$$

Within the transition zone the appropriate equation is not straightforward but the simplest approach is to extend either Darcy's or Stokes equation into this region. Beavers and Joseph (1969) verified experimentally that Darcy's equation works well. The problem with this approach is that the horizontal velocity is not continuous which is inconsistent with condition (10). As an alternative Le Bars et. al. (2006) extended Stokes equation into the transition zone which also matches well to the results of Beavers and Joseph (1969). The advantage to this method is that the velocities are continuous at the mush–liquid interface and so we use this approach here. With this method the matching conditions at the level $z = a - \delta$ between the two regions are

$$[u] = 0, \quad [w] = 0, \quad [P] = 0 \quad z = a - \delta, \tag{21}$$

where the brackets denote a jump in the enclosed quantity.

Equations (16) and (17) can be simplified by substituting in the stream function relationship and eliminating the pressure to get the following equations

$$\frac{\partial}{\partial z}\left(\frac{f'}{\Pi}\right) = 0, \tag{22}$$

$$f'''' = 0. \tag{23}$$

in the mush and liquid respectively. Finally the boundary conditions in terms of f are

$$f'(h) = 0, \qquad f(h) = \frac{W_T}{V}, \qquad f(0) = \frac{W_B}{V}, \tag{24}$$

with the following matching conditions in terms of f at $z = a - \delta$

$$[f] = 0, \qquad [f'] = 0, \qquad f'''_{+} = -\frac{f'_{-}}{\Pi}, \tag{25}$$

where $+$ denotes the liquid and $-$ the mushy layer.

2.4.2 Darcy-Brinkman formulation

An alternative to the above approach is to use a continuous formulation in terms of the Darcy-Brinkman equation

$$\nabla P = \frac{1}{1-\phi}\nabla^2 \mathbf{u} - \frac{\mathbf{u}}{\Pi}H(\phi), \tag{26}$$

which turns into Stokes equation in the liquid where the step function $\phi = 0$ and $H(\phi) = 0$. This equation has the advantage of being solvable on a single domain, which makes it favorable for problems in more than one-dimension, particularly when there are intricate changes in topography. Since fluid–fluid stresses are taken into account in this formulation the velocity is continuous at the mush–liquid interface and a transition zone does not need to be defined. Eliminating the pressure and substituting in the relationship for the stream function we get

$$f'''' = f'''\left[(\phi-1)\frac{\mathrm{d}}{\mathrm{d}z}\left(\frac{1}{1-\phi}\right)\right] + f''\left[\frac{1-\phi}{\Pi(\phi)}\right]H(\phi) + f'\left[(1-\phi)\frac{\mathrm{d}}{\mathrm{d}z}\left(\frac{H(\phi)}{\Pi(\phi)}\right)\right] \tag{27}$$

where the boundary conditions in terms of the unknown function, f, are

$$f'(h) = 0, \qquad f(h) = \frac{W_T}{V}, \qquad f(0) = \frac{W_B}{V}, \qquad f''(0) = 0. \tag{28}$$

2.5 Non-dimensionalization

We seek a steady solution in the moving reference frame ($\partial/\partial t = -V\,\partial/\partial z$) and non-dimensionalize temperature and concentration with the imposed boundary conditions as follows

$$T = x\left[-m_2 + (m_2 - m_1)\theta(z)\right], \quad C = x\left[\frac{m_2}{m} + \frac{m_1 - m_2}{m}\theta(z)\right] \tag{29}$$

We then scale the length with the width of the channel, h, and the velocity with the interface speed, V. Equations (1), (2) and (5) become

$$\theta'(f-1) - f'(\theta - \mathscr{C}) = Pe\,\theta'' - \frac{S}{x}\phi' \qquad 0 \le z \le a, \tag{30}$$

$$\frac{\mathrm{d}}{\mathrm{d}z}[(\phi-1)\theta - \mathscr{C}\phi] = f'(\theta-\mathscr{C}) - f\theta' \qquad 0 \le z \le a, \tag{31}$$

$$\theta'(f-1) - f'(\theta - \mathscr{C}) = Pe\,\theta'' \qquad a \le z \le 1, \tag{32}$$

where $Pe = k/(V\,h)$ is an inverse Peclet number and $S = L/(C_p\,h(m_2 - m_1))$ is a Stefan number. Here $\mathscr{C} = m_2/(m_2 - m_1)$ is the deviation in the horizontal temperature gradient of the lower boundary m_2 from the upper boundary m_1 and essentially gives us a measure of the temperature difference. This non-dimensional parameter could be recast in terms of solute concentrations as $\mathscr{C} = m_b/(m_b - m_1/m)$, where $m_b = m_2/m$ is the concentration of solute at the lower boundary and m_1/m is the gradient in the solute concentration at the liquidus temperature. Since we assume the channel to be infinitely long we will look for

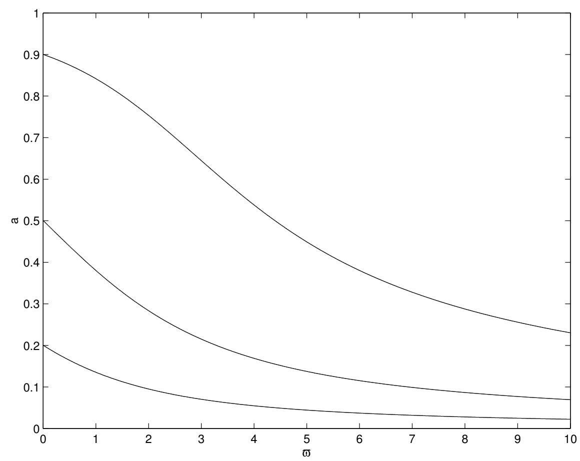

Figure 3: Mush–liquid interface position $a(\varpi, \theta)$ as a function of ϖ for $\theta_a = .2, .5$ and $.9$ corresponding to the lower, middle and upper lines respectively.

large x solutions such that, $S/x \sim 0$, which reduces our system of equations to functions of z only. The boundary conditions in the new variable θ become

$$\theta(0) = 0, \qquad \theta(1) = 1, \tag{33}$$

$$\phi = 0, \qquad [\theta] = 0, \qquad [\theta_z] = 0 \quad z = a \tag{34}$$

with the unknowns θ, ϕ, a and the velocity f determined from either the Darcy-Stokes formulation as

$$\frac{\partial}{\partial z}\left(\frac{f'}{k}\right) = 0, \qquad f'''' = 0. \tag{35}$$

$$f'(1) = 0, \qquad f(1) = W_T, \qquad f(0) = W_B. \tag{36}$$

$$[f] = 0, \qquad [f'] = 0, \qquad f_s''' = -\frac{f_D'}{D_a k}, \quad z = a - \delta. \tag{37}$$

or the Darcy-Brinkman formulation as

$$f'''' = f'''\left[(\phi - 1)\frac{\mathrm{d}}{\mathrm{d}z}\left(\frac{1}{1-\phi}\right)\right] + f''\left[\frac{1-\phi}{k(\phi)Da}\right]H(\phi) + f'\left[\frac{1-\phi}{Da}\frac{\mathrm{d}}{\mathrm{d}z}\left(\frac{H(\phi)}{k(\phi)}\right)\right], \tag{38}$$

$$f'(1) = 0, \qquad f(1) = W_T, \qquad f(0) = W_B, \qquad f''(0) = 0. \tag{39}$$

In the above equation $Da = \Pi_0/h^2$ is the Darcy number and in the liquid layer the governing equation reduces to $f'''' = 0$

3 Solutions for $W_B = W_T < V$

It is of interest to obtain a solution in which the direction of flow in the moving reference frame is from liquid to mush along a solidification boundary. In this case the condition required to determine the location of the mush–liquid interface is different from condition (10) as has been discussed previously. When the velocity of the upper and lower boundaries are equal, an exact solution is possible and its solution has interesting qualitative features that we would like to understand. In this case the governing equations, obtained by taking $f = W_B$ and $f' = 0$ in equations (30)–(32) are

$$\theta'(W_B - 1) = Pe\,\theta'' \tag{40}$$

$$\frac{\mathrm{d}}{\mathrm{d}z}[(\phi - 1)\theta - \mathscr{C}\phi] = -W_B\theta', \tag{41}$$

$$\theta'(W_B - 1) = Pe\,\theta''. \tag{42}$$

The solution to the temperature equations (40) and (42) in general are $\theta = A\exp(-z\varpi) + B$ where $\varpi = (1 - W_B)/Pe$. Applying the boundary conditions $\theta(0) = 0$, $\theta(a) = \theta_a$ and $\theta(1) = 1$ we get

$$\theta = \theta_a\,\frac{e^{-z\varpi} - 1}{e^{-a\varpi} - 1} \qquad 0 \le z \le a \tag{43}$$

$$\theta = 1 + (\theta_a - 1)\frac{e^{-z\varpi} - e^{-\varpi}}{e^{-a\varpi} - e^{-\varpi}} \qquad a \le z \le h \tag{44}$$

The position of the mush–liquid interface is determined such that the first derivatives of the temperature field are continuous, which is determined, with a little algebra, from

$$a = -\frac{1}{\varpi}\ln\left[\theta_a e^{-\varpi} + 1 - \theta_a\right]. \tag{45}$$

By integrating equation (41) and applying the boundary condition $\phi(a) = 0$ at the mush–liquid interface, we obtain

$$\phi = \frac{(1 - W_B)(\theta - \theta_a)}{\theta - \mathscr{C}}, \tag{46}$$

which gives the solid fraction as a function of the temperature profile equation (43).

In this frame of reference there is effectively a flow from the liquid to the mush in which case information about the solute concentration is transported from the upper boundary. Since there is only 1-dimensional flow with no solute diffusion the concentration in the liquid is constant and given by equation (8). This concentration translates to the mush side of the interface because of local equilibrium (see Schulze and Worster 1995) and gives a relationship for the interface temperature in non-dimensional form as

$$\theta_a = \mathscr{C}\left(1 - \frac{m\,m_t}{m_2}\right). \tag{47}$$

From this equation we can obtain a relationship for the solid fraction at the lower boundary in the form

$$\phi_B = \left(\frac{m\,m_t}{m_2} - 1\right)(1 - W_B) \tag{48}$$

which is obtained by evaluating equation (46) at $z = 0$.

The solution to equation (45) has been plotted in figure (3) as a function of the parameter ϖ for different values of the interface temperature θ_a. From these profiles it is immediately evident that the position of the mush-liquid interface decreases with ϖ which can be interpreted as an increase in the velocity W_B. In this case there is a larger transport of relatively cool fluid from below that decreases the average temperature of the system and the thickness of the mushy layer must increase.

Similarly the position of the mush–liquid interface is shown to increase with the interface temperature, which can be better understood by recasting this temperature in the form

$$\theta_a = \mathscr{C}\left(1 - \frac{m_t}{m_b}\right) = \mathscr{C}r, \tag{49}$$

where $m_b = m_2/m$ is the horizontal derivative of the concentration at the lower boundary. The first term on the right hand side gives us a measure of the temperature difference in the system in that a large value of $\mathscr{C}$ can be thought of as decreasing the temperature of the upper boundary. The second term is a ratio of the horizontal concentration gradient between the top and bottom boundaries, in which a large value of r implies a larger concentration of solute. In either case a large $\mathscr{C}$ or r indicates that the average temperature in the system is cooler and the position of the mush–liquid interface must grow into the channel in order to reduce the amount of constitutional supercooling.

4 Numerical solution

We have solved the full set of equations (30)–(32) and either the Stokes–Darcy formulation (35) or the Darcy–Brinkman formulation (38) numerically using a shooting method combined with a fourth-order Runge-Kutta ode solver. The position of the mush–liquid interface is determined such that $\phi = 0$ and $q \cdot \nabla T = 0$ as a function of the 6 parameters, W_T, W_B, $\mathscr{C}$, Da, Pe and c in our system of equations.

In figure (4) we show the general characteristics of the numerical solution for a fixed set of parameter values. Here we have used the Darcy–Brinkman formulation for consistency and reserve a discussion concerning the comparison between the two formulations for the next section. The four plots show typical profiles for the solid fraction, ϕ, temperature, θ, first derivative of the temperature, θ', vertical velocity, f and the horizontal velocity, f'. In addition we have plotted the non-dimensional form of condition (10), which is written as

$$G = \theta'(f-1) - \frac{\mathrm{d}f}{\mathrm{d}z}(\theta - \mathscr{C}), \qquad G(a) = 0. \tag{50}$$

This condition can be interpreted as the point at which the isotherms are tangent to the streamlines or equivalently the point at which horizontal advection is balanced by vertical advection of thermal energy.

4.1 Comparison between Darcy-Brinkman and Stokes-Darcy formulations

Le Bars et. al. (2006) showed that the Stokes–Darcy and Darcy–Brinkman formulations are nearly equivalent for a suitably chosen transition zone depth and in the limit of small Darcy

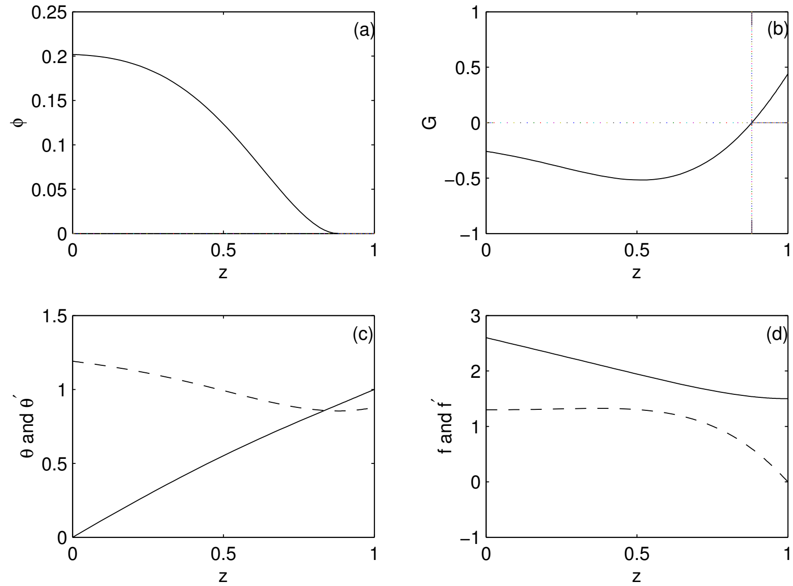

Figure 4: Numerical solution to the full set of coupled equations showing the solid fraction, ϕ, temperature, θ (solid line), temperature gradient,θ' (dashed line), advective component of the thermal energy equation, G, the vertical velocity, f (solid line) and the horizontal velocity, $-f'$ (dashed line). In plot (b) the dotted lines show the zero level and interface position. Here we use the following parameter values $\phi_B = .2019$, $\mathscr{C} = 1.667$, $W_T = 1.5$, $W_B = 2.6$ and $Pe = 1$.

number. The former method is somewhat less convenient in that it requires the solution to be broken up into two domains and the results are sensitive to the choice of scaling coefficient, c. We have plotted a typical solution in figure (5), comparing the numerical solutions for both approaches in which the best choice for the scaling coefficient is $c = 1$. As we expect the difference in the temperature, volume fraction, vertical velocity and horizontal velocity profiles are very small for the Darcy number $Da = 1 \times 10^{-4}$ chosen for comparison. In this case the transition zone thickness is $\delta = .01$, which is a small fraction of the domain height. By numerical experimentation we found that the discrepancy between the two formulations did indeed decrease with Darcy number but had a lower bound since the liquid layer $(1 - a) \rightarrow 0$ as $Da \rightarrow 0$.

4.2 Diagnostics

In this section we will compare the effect of the four parameters, Da, $\mathscr{C}$, W_T and W_B on the the mush–liquid interface position, a and the lower boundary solid fraction, ϕ_B. We fix the Peclet number to unity and use the Darcy-Brinkman formulation for consistency.

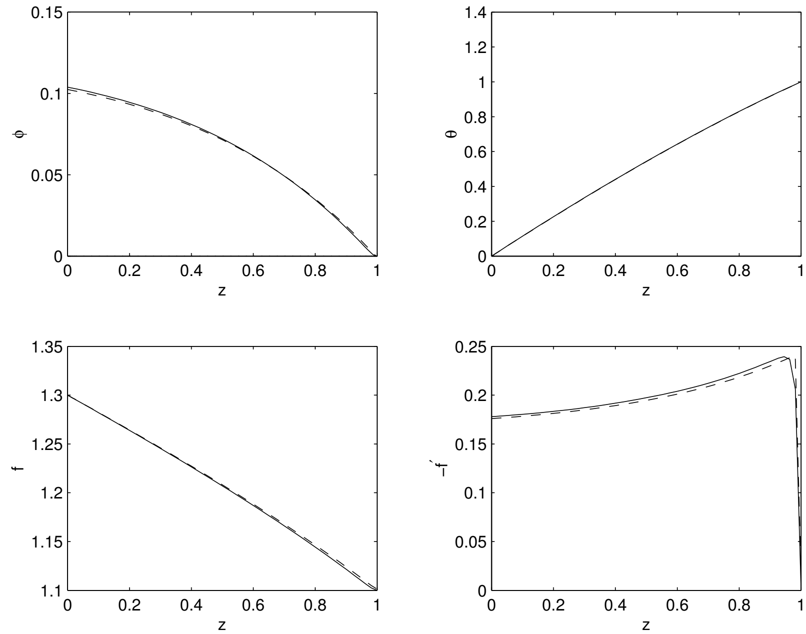

Figure 5: Comparison between the profiles for solid fraction ϕ, temperature θ, vertical velocity f and horizontal velocity f' for the Darcy-Brinkman (solid line) and Stokes-Darcy formulations (Dashed line). Here we have used the following parameter values $\mathscr{C} = 3.333$, $W_T = 1.1$, $W_B = 1.3$, $Pe = 1$ $Da = 1 \times 10^{-4}$ and $c = 1$.

4.2.1 Effect of Da

The Darcy number is a scale for the permeability in that a large Da implies less resistance to the flow and a small Da implies more resistance. Therefore we would expect that as Da decreases the flow rate would also decrease. In our case we have forced a constant velocity at the lower boundary and must conserve mass at any point in our system. The result than of a decrease in Da is to decrease the horizontal pressure gradient in the mush forcing the horizontal velocity to decrease. From figure (6) we see that as Da is made smaller the position of the mush–liquid interface must increases in order to satisfy the tangency condition (10). Since in this case the horizontal velocity is decreasing the streamlines will tend to straighten out and therefore diverge from the tangency condition. Since the vertical velocity must decrease at the end of the channel and a horizontal velocity must exist at some point in the system in order to conserve mass, there will only be sufficient curvature towards the upper boundary.

In the second graph of figure (6) we have plotted the solid fraction profiles $\phi(z)$ for three values of the Darcy number. As a consequence of the horizontal velocity decreasing with Da, the advection of thermal energy becomes smaller near the lower boundary of the mushy layer. From equation (31) we can see that the solid fraction gradient must also decrease in this region and for small Da, ϕ' approaches zero. Away from the lower boundary the horizontal velocity must increase, which leads to larger thermal advection and a steeper solid fraction gradient.

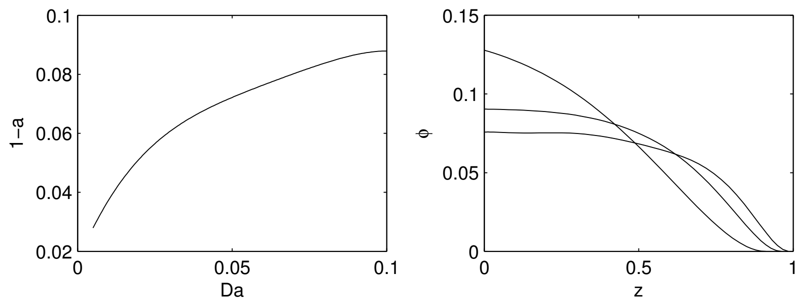

Figure 6: Numerical solution to the full set of coupled equations showing the thickness of the liquid layer (left), $1-a$ as a function of the Darcy number Da and the solid fraction profiles (right) for $Da = .002, .01$ and $.1$ corresponding to $\phi_B = .077, .09$ and $.128$ respectively. Here the other three parameter values are set to $W_T = 1.1$, $W_B = 1.6$ and $\mathscr{C} = 1.43$.

4.2.2 Effect of $\mathscr{C}$

The parameter $\mathscr{C}$ is defined as the deviation in the horizontal temperature gradient of the lower boundary m_2 from the upper boundary m_1 and really gives us a measure of the temperature difference in the system. As in the analytic solution of section (3), an increase in $\mathscr{C}$ has the effect of decreasing the thickness of the liquid layer, as seen in figure (7). Since a large value of $\mathscr{C}$ can be thought of as decreasing the temperature of the upper boundary, the average temperature in the system is lower and at steady state the mushy layer must grow further into the channel. In addition we require condition (10) to be satisfied, in which the position of the mush–liquid interface must occur at a point where the isotherms and streamlines are locally tangent. For fixed velocity boundary conditions the streamlines are to leading order independent of $\mathscr{C}$ and we can concentrate on the form of the isotherms as a function of the temperature boundary conditions. As was indirectly indicated to above, the vertical temperature gradient decreases with an increase in $\mathscr{C}$ since the difference in temperature across the channel is decreasing. Because of the form of the streamlines in the channel the position of the tangency point occurs more towards the upper boundary as the isotherms straighten out.

In addition figure (7) shows a plot of the lower boundary solid fraction as a function of $\mathscr{C}$. As this parameter is increased the thermal gradient decreases, as discussed above, but since the non-dimensional temperature gradient scales with $\mathscr{C}$, θ' actually increases. As a result of this the thermal advection term in non-dimensional form becomes larger. With reference to equation (31), we can see that in this case the solid fraction gradient increases and with it ϕ_B.

4.2.3 Effect of velocity

The velocity boundary conditions have a strong effect on the structure of the velocity field within the mush and liquid layers and is an important parameter controlling the advective flux of solute and temperature throughout the system. In figure (8) we have plotted the thickness of the liquid layer as a function of the lower boundary velocity W_B for different

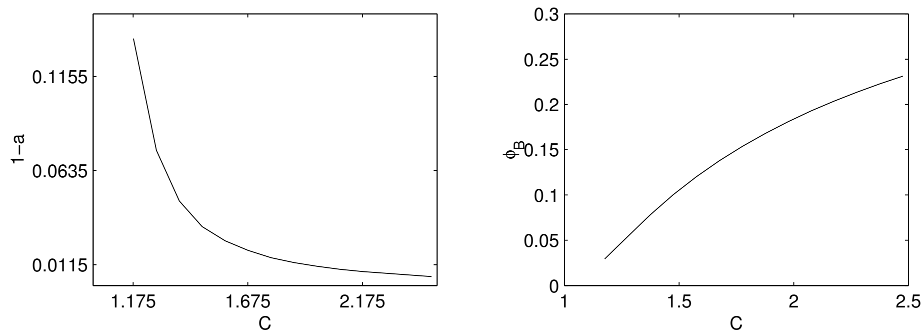

Figure 7: Numerical solution to the full set of coupled equations showing the thickness of the liquid layer (left), $1-a$ and the lower boundary solid fraction (right), ϕ_B as a function of $\mathscr{C}$. Here the other three parameter values are set to $W_T = 1.1$, $W_B = 1.6$ and $Da = .01$.

values of the upper boundary velocity W_T. This figure shows that the position of the mush–liquid interface increases with W_B, which is not surprising since we would expect there to be a larger flux of cool fluid from the bottom. In addition a larger lower boundary flux has the effect of increasing the horizontal velocity and stretching the stream lines further down the channel. As a result the mush–liquid interface is driven further upwards in order to both suppress constitutional supercooling and find a point of local tangency between the isotherms and the streamlines. By the same reasoning an increase in W_T will straighten out the streamlines and thus increase the thickness of the liquid layer as shown in figure (8).

Similarly to the discussions in section (4.2.1) and (4.2.2) an increase in lower boundary velocity acts to increase the advective transport of thermal energy. This causes the solid fraction to increase and with it the solid fraction at the lower boundary ϕ_B as shown in figure (8).

5 Conclusion

In this paper we have explored the behavior of a boundary condition originally presented by Schulze and Worster (1999). This condition requires local tangency between the isotherms and streamlines at a mush–liquid interface when the flow is from mush to liquid across a solidifying boundary. The condition naturally occurs along the chimney walls of a mushy layer and requires a two dimensional flow and temperature field to be satisfied. For this reason we constructed a simplified model that has these properties built in but that can be reduced to a one-dimensional problem. The appropriate equations to use for the velocity field within the reactive porous media can be separated into two groups, Darcy and Darcy-Brinkman, which are only equivalent in the limit of a small Darcy number. The first is a two-domain approach that requires a transition zone of order $Da^{\frac{1}{2}}$ to be defined and the second is a continuous domain approach. We solved the governing equations (31)–(32) with either the Stokes–Darcy formulation (35) or the Darcy–Brinkman formulation (38) numerically and compared solutions for both of these formulations. From comparisons of velocity, temperature and solid fraction profiles we discovered, as we expected, that the difference between the two formulations decreased as the Darcy number was made

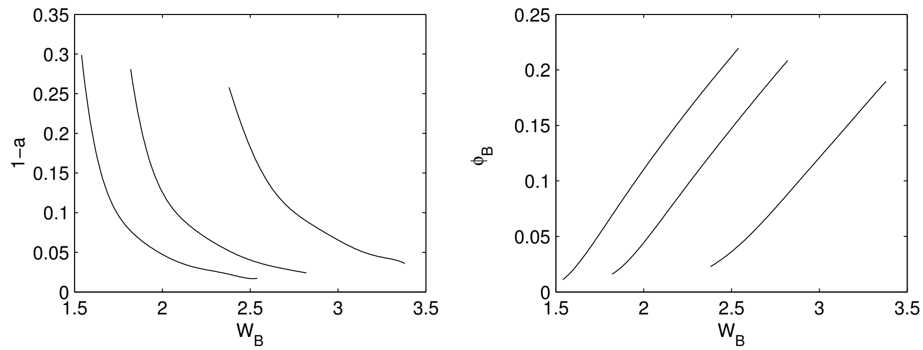

Figure 8: Numerical solution to the full set of coupled equations showing the thickness of the liquid layer (left), $1 - a$ and the lower boundary solid fraction (right), ϕ_B as a function of W_B for $W_T = 1.2, 1.3$ and 1.5. Here the other two parameter values are set to $\mathscr{C} = 1.43$ and $Da = .01$.

smaller. In addition we used the numerical solution with the Darcy-Brinkman formulation to determine the behavior of the liquid layer thickness, $1 - a$ and the lower boundary solid fraction ϕ_B as a function of the four parameters Da, $\mathscr{C}$ W_B and W_T. Since a small Darcy number tends to decrease the horizontal velocity within the mushy layer the position of the mush–liquid interface must occur near the upper boundary were mass conservation forces the streamlines to have sufficient curvature in order to satisfy the tangency condition. The lower velocity also decreases the advective transport of the thermal energy near the lower boundary which tends to suppress the solid fraction gradient. In the case of large $\mathscr{C}$, the thermal gradient decreases and therefore straightens out the isotherms, which results in the point of tangency occurring closer to the upper boundary. Because the non-dimensional form of the temperature is scaled with $\mathscr{C}$, the non-dimensional temperature gradient increases, resulting in a larger thermal advection term and therefore an increase in ϕ_B. Similarly an increase in the lower boundary velocity W_B results in a larger advection of thermal energy which lengthens out the streamlines. This forces the tangency point to occur further up the channel and increases the solid fraction at the lower boundary.

6 Future Work

The problem presented in this paper has been solved numerically for the steady state case and could lead to a larger study. The next step in the analysis would be to reformulate the equations in terms of enthalpies. Since in this case the temperature and solid fraction are consolidated into a single equation the numerical procedure would be simplified. With this new formulation we could more easily solve the transient problem numerically to gain a better understanding of how the mushy layer evolves with our current setup.

Experiments have found that tributaries form along the chimney walls, most likely due to some instability within the reactive porous medium. We have used our simplified model to examine the initiation of this feature, using linear stability analysis. In this case the basic state is the numerical solutions presented here and we look to see under what conditions the perturbations grow in time. This analysis is still in the beginning stages and still needs more refining to obtain a reasonable solution.

7 Acknowledgments

I would like to thank Grae Worster for supervising me on this project and Alan Rempel for enlightening conversations on the porch. I would also like to thank all of the staff and fellows for making this a great summer.

References

[1] M. L. Bars and M. G. Worster, *Interfacial conditions between a pure fluid and a porous medium: implications for binary alloy solidification*, J. Fluid Mech., 550 (2006), pp. 149–173.

[2] G. K. Batchelor, *An introduction to fluid dynamics*, Cambridge University Press., 1967.

[3] J. Bear, *Dynamics of Fluids in Porous Media*, Dover, 1972.

[4] G. S. Beavers and D. D. Joseph, *Boundary conditions at a naturally permeable wall*, J. Fluid Mech., 30 (1967), pp. 197–207.

[5] T. P. Schulze and M. G. Worster, *Weak convection, liquid inclusions and the formation of chimneys in mushy layers*, J. Fluid Mech., 388 (1999), pp. 197–215.

[6] ——, *A time-dependent formulation of the mushy-zone free boundary problem*, J. Fluid Mech., 541 (2005), pp. 193–202.

[7] M. G. Worster, *Convection in mushy layers*, Annu. Rev. Fluid Mech., 29 (1997), pp. 91–122.

[8] ——, *Solidification of Fluids. In Perspectives in Fluid Dynamics (ed. G.K. Batchelor, H.K. Moffat & M.G. Worster), pp. 393–446*, Cambridge University Press., 2000.